Speed control of multiple tidal turbines connected to a shared onshore converter

Simon M. Reynolds, Aristides E. Kiprakis, and Mohammad Abusara

***Abstract*—A novel control strategy is proposed for the control of two fixed pitch tidal turbines subjected to discrete flow speeds whilst interconnected in an array. It is suggested that reliability will be increased by locating all power conversion and control equipment onshore, thereby reducing Operating Expenditure (OPEX) due to offshore equipment failure. An added benefit is utilisation of a single shared export cable for both turbines, thereby reducing Capital Expenditure (CAPEX). By lowering the cost of installing and maintaining an array it is anticipated that the commercial viability of the project will be enhanced. Speed regulation of Induction Generators (IG) is carried out through Field Oriented Control (FOC) with reference torque calculated by Optimal Torque Control (OTC). This provides Maximum Power Point Tracking (MPPT) whilst allowing individual generators to run at different speeds by varying the Tip Speed Ratio (TSR) of each turbine. Estimated current waveforms calculated via FOC are averaged between both turbines and fed to a Pulse Width Modulation (PWM) generator for comparison against actual averaged currents from both generators. A shared Insulated Gate Bipolar Transistor (IGBT) rectifier is controlled by PWM pulses to maintain the currents of both generators in phase. A Simulink model was constructed to test this control strategy; the results generated demonstrate that two turbines can be operated in parallel, whilst still maintaining an acceptable level of efficiency.**

***Keywords* – Array, control, electrical, induction generator, tidal energy, tidal turbine.**

I. Introduction

With mounting evidence about the impact of climate change it is becoming increasingly critical that renewable energy is used to displace electricity generation by conventional fossil fuels. Electricity generation in the UK was responsible for the release of 144 MtCO2e in 2015 [1]. In 2015, renewables generated 24.6% of the UK's electricity demand, at 83.55 TWh; Wave and Tidal combined represented just 0.0024% of this amount at 2 GWh [2]. It has been estimated that the amount of energy that could be practically extracted from the UK Tidal Stream resource is approximately 20TWh [3]. This would provide around 6% of the UK's 339 TWh electricity demand as it currently stands [2].

As Tidal Energy matures as a technology, the need to address cost effectiveness and reliability becomes increasingly important. For the sector to compete with existing energy generation technologies, it is clear that arrays will be required to provide economies of scale, as demonstrated in the Wind energy sector. The optimum topology for these arrays has not yet been established, in part due to the added complication of carrying out routine repair and maintenance operations on equipment located subsea. Wind turbine reliability studies have consistently shown that the electrical control and power conversion equipment is amongst the components most likely to fail [4]. Given the similarity of the components used in Wind and Tidal energy converters it is safe to assume that Tidal arrays will suffer from comparable rates of failure. Therefore the advantages of locating power conversion and control equipment on shore are obvious: greatly improved accessibility and therefore reduced downtime in the event of failures.

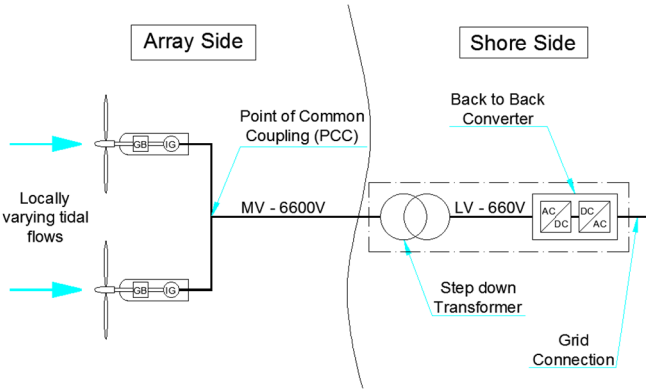

Fig. 1. Proposed tidal turbine array connection and power conversion equipment topology

Another issue affecting the competitiveness of tidal energy is high upfront installation costs, a significant proportion of which comes from the export cables, both in material and vessel operating costs.

1228 – Grid integration, power take-off and control

"This work was supported in part by the Industrial Doctoral Centre for Offshore Renewable Energy (IDCORE) and the University of Edinburgh in conjunction with the Energy Technologies Institute (ETI) and the Research Councils UK Energy programme (Grant number EP/J500847/1)"

S. M. Reynolds is with the Industrial Doctoral Centre for Offshore Renewable Energy (IDCORE), The University of Edinburgh, King's Buildings, West Mains Road, Edinburgh, EH9 3JG, UK (e-mail: s.reynolds@ed.ac.uk).

A. E. Kiprakis. is with the Institute for Energy Systems, The University of Edinburgh, King's Buildings, West Mains Road, Edinburgh, EH9 3JG, UK (e-mail: aristides.kiprakis@ed.ac.uk).

M. Abusara is with the Renewable Energy Research Group, The University of Exeter, Penryn Campus, Falmouth, TR10 9FE, UK (e-mail: m.abusara@exeter.ac.uk).

Consequently, an alternative array configuration which uses shared export cables for multiple turbines, together with onshore power conversion equipment is attractive, as shown in Fig. 1.

Naturally there are challenges to the effective implementation of such a strategy and the control methodology utilised is key to resolving these difficulties. This paper aims to briefly explain the theory behind the principles for the proposed control strategy and discuss the results of the modelling used to validate them.

Related research has been carried out in this area previously, with arrays modelled using both Wind and Tidal turbines. However, there are notable differences between this prior work and the research presented in this paper. Sousounis et al. [5] focus on the analysis of controlling tidal turbines using long distance drives located on shore. Importantly, the shared converter topology is different, with each turbine connected via single cables to an individual rectifier, and multiple rectifiers sharing a single inverter. Elliott et al. [6] propose a scheme for clustering multiple wind turbines together via relatively short cables to a common converter located offshore. Trilla et al. [7] suggest connection of multiple turbines to a common generator side converter located offshore, with a long distance HVDC link back to shore where the grid side converter is located. Other research by Chen at al. [8], and the Offshore Renewable Energy Catapult [9], illustrate turbine control topologies and options for array interconnection. These do not cover the method presented in this paper, further demonstrating the novelty of the research.

The key novel aspect of the research presented in this paper is the effective control of two induction machines via a single export cable with a shared onshore converter.

II. Single Tidal Turbine Modelling

This section will briefly describe the modelling approach utilised and define the key calculations used. A model was built in Simulink to represent a single tidal turbine with a gearbox and a 400kW, 6.6kV Squirrel Cage Induction Generator (SCIG). The SCIG is connected to a generator side 660V 3 arm Insulated Gate Bipolar Transistor (IGBT) rectifier via a 2km long three phase cable and transformer.

Data obtained via Acoustic Doppler Current Profiler (ADCP) measurement of Ramsey Sound in Wales was analysed using the WinADCP software package. This ADCP data was obtained in a series of 42 bins taken through the water column to give the full structure of the shear profile and turbulence intensity at the deployment site. The bins which span the diameter of the rotor were used and a median value obtained across them to eliminate outliers. Although a full tidal cycle is 12 hours and 25 minutes between low tides, a 12 hour range was chosen, for the sake of simplicity and because the missing time covered very low flow speeds around slack flow. The tidal cycle used starts at slack flow and reaches the peak flow for that day, in this case approximately 2.65m/s, before ramping back down to slack flow. The flow was averaged across segments of time to eliminate some of the very rapid turbulence fluctuations that would otherwise be seen in the model due to the relatively short run time used, solely for practical constraints. This gave a realistically varying flow, albeit with slower turbulence variations to accommodate the modelling approach requirements.

A. Turbine, Gearbox and Generator Mechanical Parameters

The mechanical characteristics of the fixed pitch turbine and induction generator were defined in the Simulink model to ensure it was as representative as possible. These included rotor and generator inertia, together with shaft stiffness; the relevant parameters given in Table I below can be used to define turbine performance.

TABLE I
KEY PARAMETERS FOR THE DELTASTREAM TURBINE

Symbol	Quantity	Value
Gbr	Gearbox Ratio	1:72
η_{Gb}	Gearbox Efficiency	96%
J1	Generator Inertia	67.6 kg.m^2
J2	Turbine Inertia	8.43 kg.m^2
K	Shaft Stiffness	600000 N.m.rad^{-1}
C_p^{max}	Maximum C_p	0.40481
TSR^{max}	Maximum TSR	3
R	Turbine Radius	12m

$$TSR = \frac{\omega \times R}{v} \quad (1)$$

Where:

ω = Turbine Speed (rad.s^{-1})
v = Water Speed (m.s^{-1})

Consequently, power extracted by the turbine from the water:

$$P = 0.5 \times \rho \times A \times v^3 \times C_p \text{ (W)} \quad (2)$$

Where:

A = Turbine Area (m^2)
ρ = Water Density (kg.m^{-3})

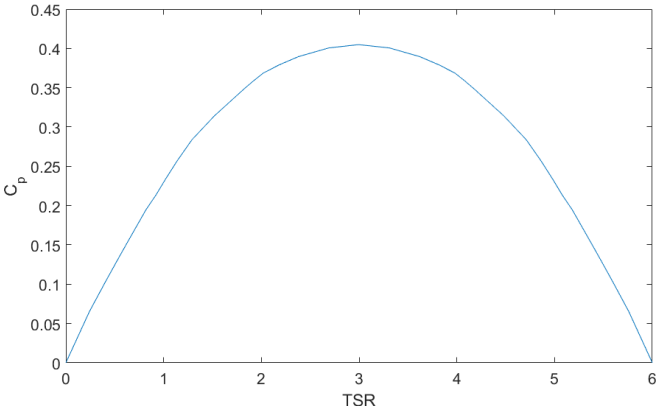

Fig. 2. Turbine C_p vs TSR

A lookup table within the turbine model provides reference C_p values for the TSR, as shown in Fig. 2, at which the turbine is operating given the flow speed it experiences.

B. Generator Control

At this stage of the research, the grid side converter is simply represented by a capacitor with a fixed DC voltage; further research would aim to provide full control via a second IGBT device. The Fixed DC reference voltage is calculated by [10]:

$$V_{dc}{}^{*} = \frac{\sqrt{6} \times V_{ail}}{m_a} \tag{3}$$

Where:

$$V_{ail} = \text{Grid Line Voltage} = \frac{V_{aip}}{\sqrt{3}} \tag{4}$$

Where: m_a = Modulation Index = 0.85; V_{aip} = Grid Phase Voltage = 660V; giving $V_{dc}{}^{*}$ = 1098.1 V.

The control scheme utilised within the model is the direct Field Oriented Control (FOC) method, coupled with Optimal Torque Control (OTC). This allows for Maximum Power Point Tracking (MPPT), thereby ensuring that the turbine operates as close to maximum efficiency as possible. An advantage of the FOC method is that the only feedback signals required are from a generator speed sensor and generator three phase current. There is no need to measure flow speed, something that can prove difficult to do accurately and reliably.

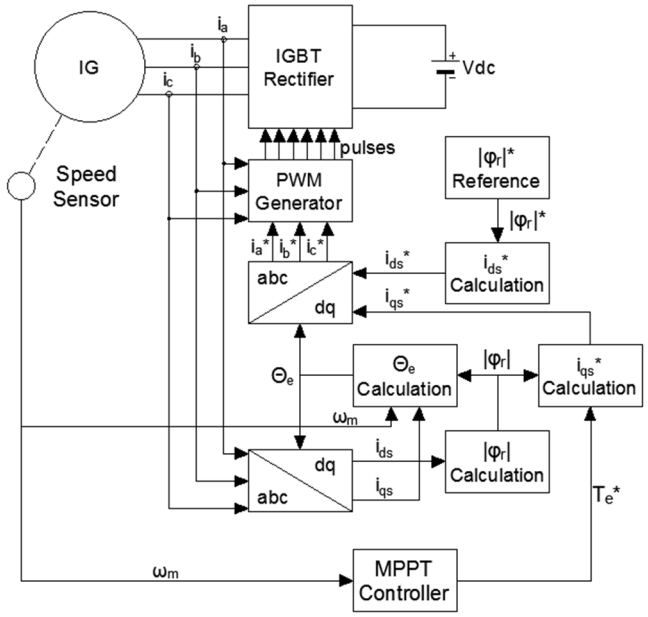

Fig. 3. FOC scheme used for individual control of IGs

Fig. 3 visually explains the methodology for controlling the IGBT using current and speed measurement, via the FOC scheme mentioned earlier. The FOC method uses a rotating dq axis reference frame to estimate the three phase current at which the generator should operate for any desired rotor speed.

Estimated d Axis Current ($i_{ds}{}^{*}$):

$$i_{ds}{}^{*} = \frac{|\varphi_r|^{*}}{L_m} \tag{5}$$

Estimated q Axis Current ($i_{qs}{}^{*}$):

$$i_{qs}{}^{*} = \frac{2}{3} \times \frac{2}{p} \times \frac{L_r}{L_m} \times \frac{T_e{}^{*}}{|\varphi_r|} \tag{6}$$

Where:

$|\varphi_r|^{*}$ = Reference Rotor Flux Linkage (Wb – turns)

$$|\varphi_r|^{*} = \sqrt{2} \times \Lambda_r \tag{7}$$

p = Number of Poles
$T_e{}^{*}$ = Generator Reference Torque (N.m)
L_r = Rotor Self Inductance (H)

$$L_r = L_{lr} + L_m \tag{8}$$

L_m = Magnetising Inductance (H)

$$L_m = \frac{jX_m}{\omega_s} \tag{9}$$

$|\varphi_r|$ = Rotor Flux Linkage (Wb – turns)

$$|\varphi_r| = \frac{L_m \times i_{ds}}{1 + \tau_r \times s} \tag{10}$$

Where:

Λ_r = Polar RMS Rotor Flux Linkage Real Component (Wb)
L_{lr} = Rotor Leakage Inductance (H)

$$L_{lr} = \frac{jX_{lr}}{\omega_s} \tag{11}$$

jX_m = Magnetising Reactance (Ω)
jX_{lr} = Rotor Leakage Reactance (Ω)
ω_s = Synchronous Angular Velocity (rad.s^{-1})

$$\omega_s = 2 \times \pi \times f_s \tag{12}$$

τ_r = Rotor Time Constant (s)

$$\tau_r = \frac{L_r}{R_r} \tag{13}$$

s = Time (s)
i_{ds} = Measured d Axis Current (A)

Where:

R_r = Rotor Resistance (Ω)

f_s = Stator Frequency = $\frac{n_r \times p}{120}$ (Hz)

$$f_s = \frac{n_r \times p}{120} \tag{14}$$

n_r = Generator Rated Speed (rpm)

The three phase current measured at the generator is fed into a dq axis transformation block to yield the actual stator d (i_{ds}) and q (i_{qs}) axis currents. The estimated currents are compared with the measured currents and a Pulse Width Modulation (PWM) generator used to create pulses for control of the IGBT rectifier.

The key variable that must first be established for the control system to function within its rated parameters is the reference rotor flux linkage ($|\varphi_r|^*$). This is critical because the estimated parameter of i_{ds}^* and hence the reference three phase currents that are used for comparison with the measured values in the simulation are derived from it. Otherwise the simulation will never reach initial convergence since the estimated parameter will be too different from the one calculated in the model. Before this can be done, the generator equivalent circuit values must be determined since these are required to calculate the rotor flux reference; the equivalent circuit diagram with its key parameters can be seen in Fig. 4 below.

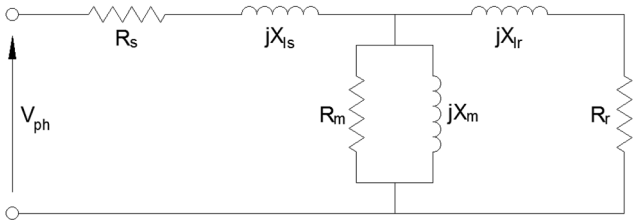

Fig. 4. Induction generator equivalent circuit

The original PU values were taken from the generator data sheet and multiplied by a new base impedance of 97.574 Ω, calculated using equation (15).

$$Z_{base} = \frac{(V_{ll})^2}{S} \tag{15}$$

Where:

V_{ll} = Line to Line Voltage (V)
S = Apparent Power (VA)

This was necessary since the induction machine block used in the Simulink model was in SI rather than PU units; the calculation results are shown in Table II. Using these values, the remaining parameters for inductance can be calculated with equations (8), (9) & (11).

TABLE II
SI VALUES FOR THE DELTASTREAM INDUCTION GENERATOR

Symbol	Quantity	Value
V_{ll}	Line to Line Voltage	6.6 kV
S	Apparent Power	446.4 kVA
R_s	Stator Resistance	0.9385 Ω
jX_{ls}	Stator Leakage Reactance	6.2597 Ω
R_m	Magnetising Resistance	15888.3162 Ω
jX_m	Magnetising Reactance	257.8399 Ω
jX_{lr}	Rotor Leakage Reactance	6.2788 Ω
R_r	Rotor Resistance	5.7153 Ω
s	Slip	0.0513

Using the values obtained from equations (5) to (14) above, the reference rotor flux linkage can be determined using equation (7). Full derivation of this equation is not presented in this paper for the sake of brevity.

Finally, the generator reference torque is calculated using the OTC method mentioned previously, where the measured speed of the generator is squared and multiplied by a torque gain term [10]:

$$T_e^* = \omega_m^2 \times k_T \tag{16}$$

Where:

ω_m = Generator Mechanical Speed (rad. s^{-1})

$$k_T = \left(0.5 \times \rho \times \pi \times R^5 \frac{C_p^{max}}{TSR^{max^3} \times Gbr^3}\right) \tag{17}$$

This calculation is carried out within the MPPT controller block shown in Fig. 3 above and is used to dynamically calculate i_{qs}^* as per equation (6).

C. Harmonic Filter

Initial iterations of the model did not utilise any three phase harmonic filters, which created problems with the model results due to the length of the cables involved and the remote nature of the power conversion equipment.

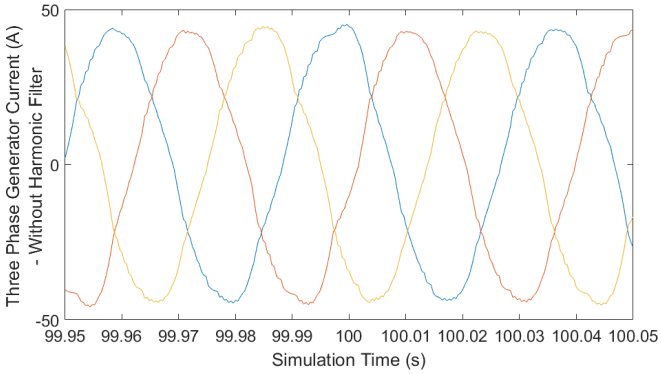

Fig. 5. Three phase current waveforms without harmonic filter

It is suggested that the current pulses transmitted by the IGBT rectifier to control the generator cause distortion of the output current waveforms due to reflections at the end of the long export cable [5].

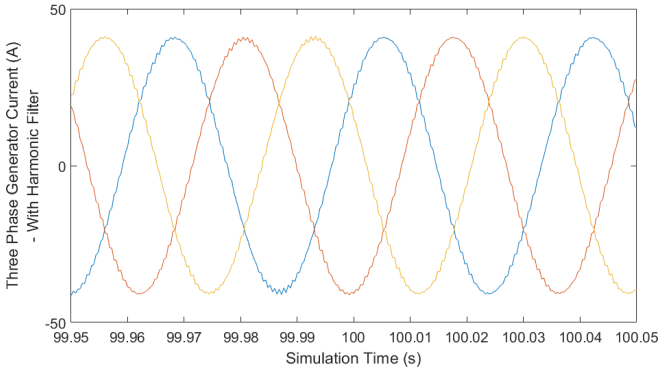

Fig. 6. Three phase current waveforms with harmonic filter

Subsequent experimentation with filters found that filtering out the third order harmonic using an 8MVA

filter after the cable, but before the transformer yielded improved results, with significantly smoother current waveforms. Fig. 5 and Fig. 6 demonstrate the before and after results for the three phase current waveforms at a sample time interval from the simulation, when the harmonic filter described above was used in the model.

There is a clear improvement in the shape of the sine waves and reduced noise in the waves themselves. The use of the filter also gave results which exhibited closer correlation to the original data obtained from Tidal Energy Ltd (TEL), suggesting that the control scheme functions better, presumably due to less signal interference over the long export cable.

Having built the single turbine model, the next stage was to construct a twin turbine model against which to compare the initial results obtained from the first model. The second key stage of the research will be described in section III below.

III. Tidal Turbine Array Modelling

A number of different methods were investigated for controlling two turbines with parallel connected generators, before narrowing it down to the two most promising options. The first option involved using a single shared controller to measure the speed of both rotors and designate the fastest as the lead turbine using if logic control. The lead turbine three phase current was then fed to the PWM controller for comparison with the estimated current from the VOC block. Both turbine speeds were averaged to feed into the OTC block to generate the torque reference for the VOC block. This methodology allowed the faster turbine to overspeed slightly, i.e. to run at faster than optimal TSR, and the second turbine to run below optimal TSR.

Whilst this methodology produced the desired result in terms of parallel control, the disparity in the two turbine speeds was greater than would have been liked. The second control option was chosen for presentation in this paper as it allows both turbines to run at consistently higher C_p values throughout the flow range.

The tidal turbine array model is simply an expansion of the single model, with the turbine, generator and controllers duplicated. The two turbines were then connected in parallel to the shared cable, transformer and IGBT rectifier, with the addition of a current averaging block. The basic model schematic is detailed in Fig. 8 for clarity.

The same tidal flow was used as for the single turbine model, with the first turbine given a 5% flow reduction to account for flow disparity across the array, whilst the second turbine saw a 2 second time delay to create a phase shift in the flow signal as shown in Fig. 7.

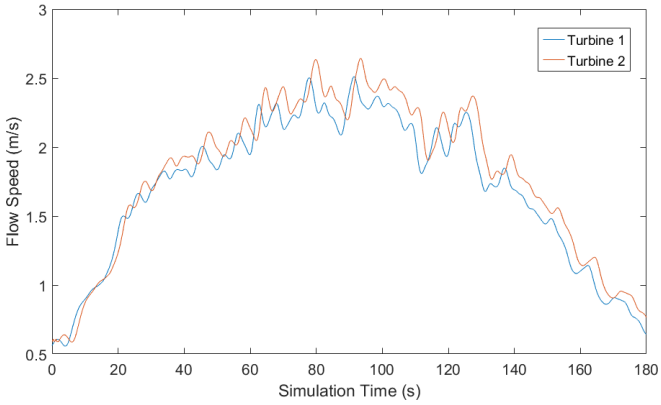

Fig. 7. Twin turbine flow speed against simulation time

Measurements are taken from each turbine as described previously, with rotor speed fed into an individual OTC block for each turbine. Generator reference torque is calculated as before and fed into a separate FOC block along with measured stator currents to generate estimated three phase currents. The estimated and measured three phase currents are then split into single phase signals and the mean calculated between each turbine. These values are then combined back into three phase signals and the mean and measured currents then sent to the PWM generator to produce pulses for control of the shared IGBT rectifier. Once again, the grid side converter is omitted, with a fixed DC voltage set instead.

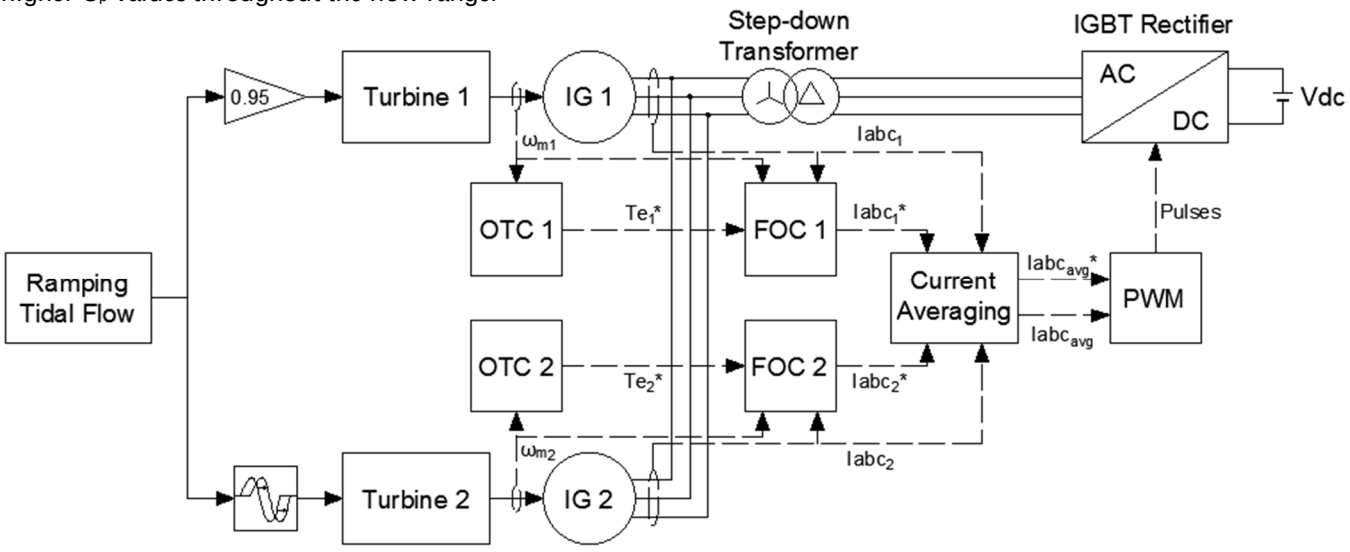

Fig. 8. Interconnected twin turbine array with shared IGBT Rectifier

IV. Results

D. *Single Turbine*

Once the single turbine model had been created to match the TEL system, from rotor to IGBT converter, initial results were generated to establish whether the model was accurately representing the system's performance.

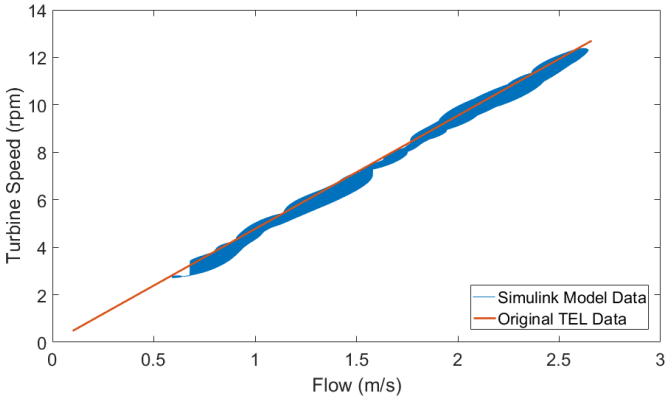

Fig. 9. Turbine speed against flow with TEL data overlaid - single model

As can be seen in Fig. 9, correlation is excellent for turbine speed, and extremely close for generator power (Fig. 10). It is worth noting that the Simulink results were generated from the fluctuating flow regime described previously, whilst the TEL data presented was developed from an idealised ramping flow. Turbulence intensity was not accounted for in the TEL data, and calculations were carried out in Excel using simple steady state equations. Importantly, the generator power is only calculated based on efficiency at different speeds rather than through the electrical parameters as used in the Simulink model.

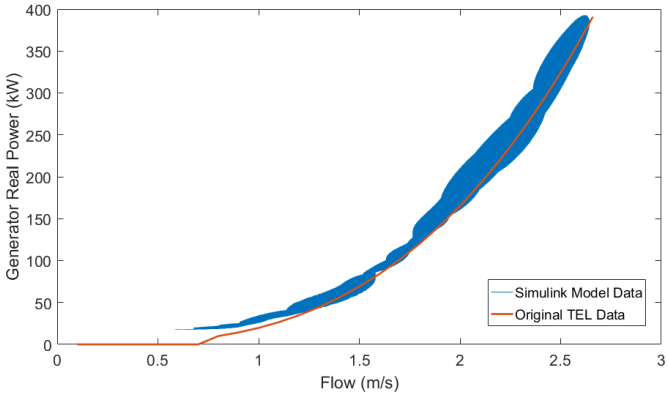

Fig. 10. Generator real power against flow with TEL data overlaid - single model

The turbulent flow regime used in the Simulink model may account for the difference in the power curves, particularly at higher flows as the generator will respond retroactively to the changing flow regime. The speed curve also displays a relatively noisy response with a reasonable amount of scatter; again, this will be due to the difference in the way the data was generated. In addition, the Simulink model ramps up and back down, meaning the generator response will be different as it accelerates and decelerates with the flow. The spread of points increases noticeably at higher flow speeds, as would be expected due to turbulent effects magnifying the variation due to power increasing by the cube of the flow.

In any instance, the correlation is good and proves the basic function of the model in simulating the TEL system, which meant that further analysis could be conducted under the assumption that the model is representative.

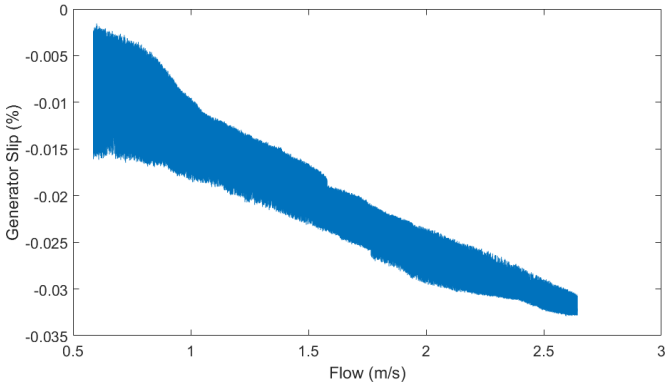

Fig. 11. Generator slip against flow - single model

Fig. 11 demonstrates generator slip increasing with flow speed, as would be expected whilst the turbine torque correspondingly increases. At higher flow speeds, the rotor mechanical frequency increases faster than the stator electrical frequency, leading to higher slip, since:

$$s = \frac{(N_s - N_m)}{N_m} \times 100 = \text{slip (\%)} \qquad (18)$$

Where:

N_s = Synchronous Speed (rpm)
N_m = Mechanical Speed (rpm)

E. *Twin Turbine*

Having established that the single model was closely representative of the original TEL data for the turbine, results were generated from the twin turbine model. Where possible, data was plotted for both turbines on the same axes to provide a visual comparison; in some instances clarity of representation prevented this and data for each turbine was plotted separately. Fitted curves were generated from the plots created from the single turbine model data shown previously and saved with their own axes as standalone objects in Matlab. This allowed them to be plotted together with the data generated from the twin turbine model to give a visual comparison of the difference in the values obtained from both models. Generally each curve used a 3rd order polynomial function as these provided the closest fit for each data set, with R^2 values of 0.98 or higher.

It can be seen in Fig. 12 that turbine 1 has to effectively overspeed slightly, which tallies with the reduced C_p figures seen for this turbine when running the Simulink model. This is because the turbine is operating at a lower than optimal TSR, thereby moving away from its

maximum efficiency point. As turbine 1 speed is higher than turbine 2, torque must necessarily be lower to produce the same amount of power, since:

$$P = \tau \times \omega = \text{Power (W)} \quad (19)$$

Where:

τ = Torque (N.m)
ω = Rotational Speed (rad.s^{-1})

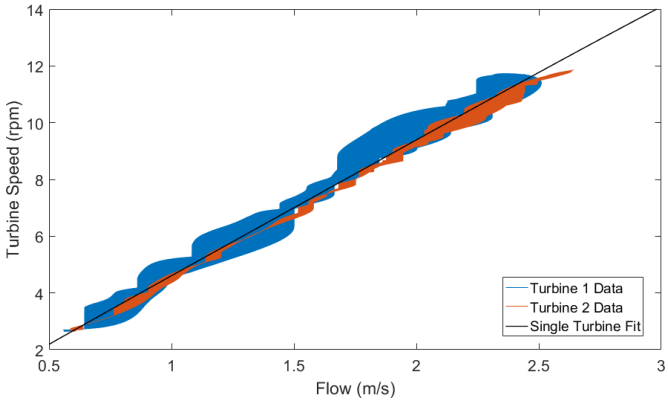

Fig. 12. Turbine speed against flow with curve fit - twin model

The MPPT control scheme is driving this behaviour, by matching power through changing torque to correlate with the higher turbine speed as necessary. Since the two turbines are controlled by the average of their real and estimated three phase currents, there should be no reason for either turbine to act as a slave to the other except when the flow it is experiencing is lower than the other. It would be worth checking this hypothesis, to see if the reverse is true, when the first turbine is subjected to higher flows than the second and see if the speed is higher for the second turbine.

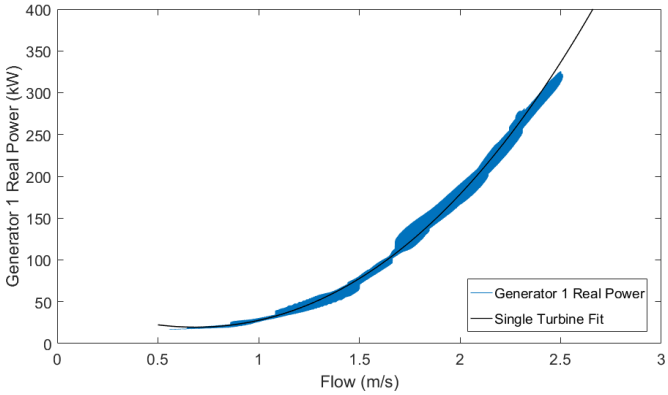

Fig. 13. Generator 1 real power against flow with curve fit - twin model

Generator electrical power is very close to the single turbine model fit for both generators, despite the fact that the flow is lower for turbine 1. This provides confidence that the control scheme is optimising power output for both turbines as far as possible given the trade-off from operating both in parallel. Generator 2 is producing slightly more power throughout the flow range than generator 1, as would be expected, despite the fact that turbine power, i.e. shaft power to the generator is almost the same. This is because the generators are operating at different points on their efficiency curves, since rotational speed is not the same, so are therefore seeing different electrical power out. Further work is required to fully establish the reasons for this behaviour and to quantify the difference in power produced. Regardless, the reduction in power generated in the twin turbine model is shown to be modest.

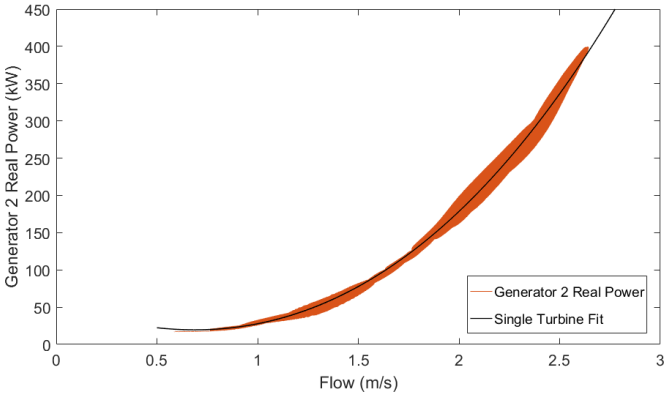

Fig. 14. Generator 2 real power against flow with curve fit - twin model

For both generators, the spread of points on the power graphs is noticeably lower than for the single turbine model. The current and voltage for each is in phase to allow them to be controlled via the shared cable and rectifier, although the magnitudes are different. The stator frequencies of both machines must remain the same for the current and voltage from each machine to remain in phase with each other; however, the rotor speeds are different, therefore slip must increase to account for this.

It is therefore proposed that the current averaging scheme is having an additional, beneficial effect, in that it is reducing the influence that extreme flow speeds, i.e. outliers, have on the input speed to the generator. When looking at Fig. 7, it can be seen that the flow for each turbine is only ever briefly at the same magnitude due to the way the two flow regimes have been configured. Therefore the calculations carried out in the current averaging block, which rely on speed feedback from the turbine, will always be attempting to meet the difference between the flows. The outcome of this is to smooth the turbulent fluctuations in the flow, to generate cleaner electrical power output; this can be clearly seen when visually comparing Fig. 13 and Fig. 14 against Fig. 10.

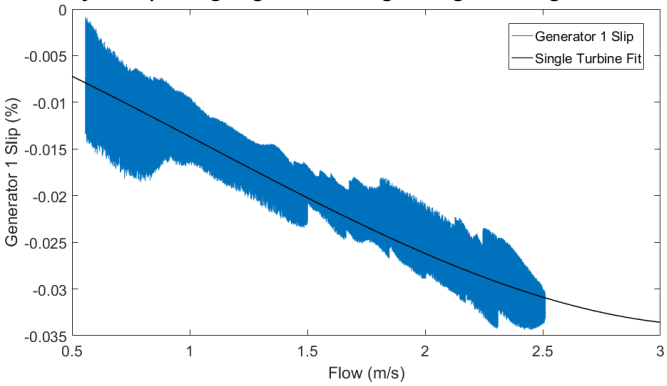

Fig. 15. Generator 1 slip against flow with curve fit - twin model

Interestingly, the plots shown in Fig. 15 and Fig. 16, demonstrate that slip against flow does not have a noticeably wider spread of points, except at higher flows. They are less uniform however, which is due to the mismatched rotor speed of the generators, as a consequence of the different flow speeds. The peaks and troughs correspond to points at which one turbine or the other changes from being at a higher or lower speed than the other due to the flow speeds having different magnitude and phase.

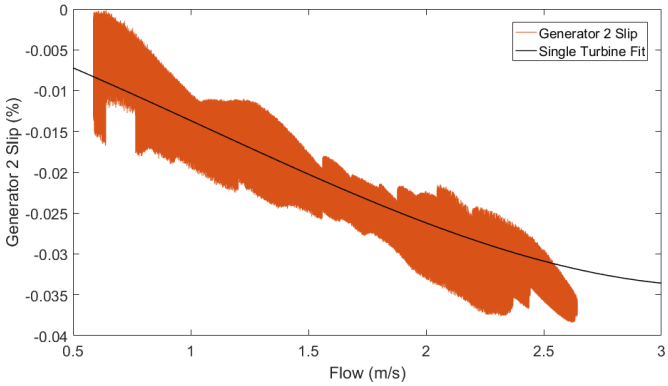

Fig. 16. Generator 2 slip against flow with curve fit - twin model

As discussed previously, the stator frequencies for both generators must be the same, i.e. stator voltage and current must be in phase for them to operate in parallel and export power at the same time. However, the mechanical speed and torque of each generator will be different as a result of the flow difference between them, leading to different slip values for each. In other words, when the rotor speeds are different, the only way for the synchronous speed to remain the same for both generators is for the amount of slip to vary between the two machines.

A final thing to take away from these graphs is that slip remains sensible for both generators, well within the maximum given limit of 0.0513 specified in the original generator parameters (Table II). This gives further confidence that it is feasible for the scheme to control two generators when flow is at a reasonable differential. However it remains to be seen what would happen if flow speeds were separated further, or more than two generators were connected in parallel.

V. Conclusions

The results presented in this paper show a strong correlation between the single turbine Simulink model and the original TEL data for the DeltaStream turbine. The data obtained from the model is noticeably noisier than the original TEL data, but this it to be expected given the difference in the way it was generated. The exact details of the original TEL control methodology for the generator are unknown since it is proprietary information, therefore it cannot be stated that exactly the same approach was used in the Simulink model. Nonetheless, it yields very similar results, particularly for the factor which in many ways is the most important: generator electrical power output. Sensible results for generator slip were obtained, corresponding well with the available generator data, thereby proving that the control strategy is working effectively to keep within operational limits even when using a turbulent flow regime. The slight divergence between the Simulink model data and the original TEL data can be explained with the reasons given above: using a turbulent flow regime instead of steady state calculations, and a control strategy that is unlikely to be identical.

Given that the single turbine model was established to be representative of the TEL system, evaluation of the twin turbine model was carried out to provide comparative results and demonstrate the function of the new control strategy. The twin turbine model data was plotted with fitted curves created from the single turbine model to provide a simple visual comparison of the closeness of the data. In each instance, correlation was extremely close, giving confidence that despite the addition of a second turbine with a different flow, the control methodology was able to operate both generators within the limits of their normal operating conditions. One point of note is that slip for both generators is noticeably higher than for the single turbine as would be expected. Given the difference in turbine speeds, slip must vary whilst the stator frequencies remain equal to allow current and voltage to remain in phase. Electrical power out was also not significantly lower than the single model, suggesting that efficiency losses are minimal.

It should also be reiterated that the results suggest that whichever turbine experiences higher flow speed at a given time, is given preference by the controller over the turbine with slower flow. At this point in the research, not enough data has been presented to fully evaluate this behaviour and establish what, if any, effect it will have on the efficiency of the parallel connected array. This operational mode may also be a function of the flow speed difference, since the slower turbine is forced to overspeed, meaning that the slower turbine then operates further from its optimum TSR with a corresponding drop in C_p. This is necessary to allow stator electrical frequency to remain the same for both generators so that current and voltage can remain in phase. The overspeed behaviour is due to limitations in the maximum difference in slip that the two generators are able to accommodate before they are pushed beyond their operational parameters.

The research presented in this paper demonstrates that it is possible to reduce the number of export cables in an array by electrically controlling two tidal turbines in parallel, even when using a shared onshore converter.

VI. Further Work

The overspeed behaviour exhibited by the slower turbine in the array requires further investigation to fully understand the reasons for this operational mode.

It would be beneficial to further optimise the control parameters, as currently they are relatively simple and

although the control scheme functions as desired, there could be room for further efficiency gains. In particular, it would be desirable to add an inverter to the current configuration of the converter to give full control over the grid side of the array.

More work is required to optimise the parameters of the generator harmonic filter, whilst the addition of a second filter on the grid side may improve overall array performance.

It is proposed that analysis should be carried out into the difference in energy yield between the single turbine and twin turbine models to quantify the efficiency loss between them.

Finally, it would be of great interest to establish how many parallel generators could be connected using the control scheme, and at what maximum flow differential.

ACKNOWLEDGMENT

The authors would like to thank the Industrial Doctoral Centre for Offshore Renewable Energy (IDCORE) and the University of Edinburgh for funding this project in conjunction with the Energy Technologies Institute (ETI) and the Research Councils UK Energy programme (Grant number EP/J500847/1).

REFERENCES

[1] Department for Business, Energy & Industrial Strategy, "2015 UK Greenhouse Gas Emissions, Final Figures", London, Stat. Rel. Feb 7, 2017.

[2] Department for Business, Energy & Industrial Strategy, "Digest of United Kingdom Energy Statistics 2016", London, July 2016.

[3] Carbon Trust," UK Tidal Current Resource & Economics", London, June 2011.

[4] H. Guo, S. Watson, P. Tavner and J. Xiang, "Reliability analysis for wind turbines with incomplete failure data collected from after the date of initial installation", *Reliability Engineering & System Safety,* vol. 94, Iss. 6, pp 1057-1063, June 2009

[5] M. C. Sousounis, J. K. H. Shek and M. A. Mueller, "Modelling, control and frequency domain analysis of a tidal current conversion system with onshore converters", in *Proc. IET Renewable Power Generation*, pp 1-8, July 2015.

[6] D. W. Elliott, S. J. Finney and C. Booth, "Single converter interface for a cluster of offshore wind turbines", in *Proc. IET Conference on Renewable Power Generation*, pp 1-6, Sep 2011.

[7] L. Trilla, O. Gomis-Bellmunt, A. Junyent-Ferre, A. E. Alvarez and A. Sudria-Andreu, "Control of a squirrel cage induction generator wind farm connected to a single power converter", in *Proc. Universities Power Engineering Conference*, Aug 2010.

[8] Chen, H., Ait-Ahmed, N., Zaim, E., & Machmoum, M., "Marine Tidal Current Systems: state of the art", in *Proc. IEEE International Symposium on Industrial Electronics,* pp 1431-1437, 2012.

[9] Offshore Renewable Energy Catapult, *Marine Energy Electrical Architecture: Report 3: Optimum Electrical Array Architectures,* Glasgow, UK: ORE Catapult, 2015.

[10] B. Wu, Y. Lang, N, Zargari, A. Kouro, *Power Conversion and Control of Wind Energy Systems*, Hoboken, USA: John Wiley & Sons Inc, 2011.

[11] V. Yaramasu, B. Wu, *Model Predictive Control of Wind Energy Conversion Systems*, Hoboken, USA: John Wiley & Sons Inc., 2017.